

# Solitons explore the quantum classical boundary

Aparna Sreedharan,<sup>1</sup> Sarthak Choudhury,<sup>1</sup> Rick Mukherjee,<sup>1,2</sup> Alexey Streltsov,<sup>3,4</sup> and Sebastian Wüster<sup>1</sup>

<sup>1</sup>Department of Physics, Indian Institute of Science Education and Research (IISER), Bhopal, Madhya Pradesh 462066, India

<sup>2</sup>Department of Physics, Imperial College, SW7 2AZ, London, UK

<sup>3</sup>Theoretische Chemie, Physikalisch-Chemisches Institut, Universität Heidelberg, Im Neuenheimer Feld 229, D-69120 Heidelberg, Germany

<sup>4</sup>SAP Deep Learning Center of Excellence and Machine Learning Research SAP SE, Dietmar-Hopp-Allee 16, 69190 Walldorf, Germany

It is an open fundamental question how the classical appearance of our environment arises from the underlying quantum many-body theory. We propose that the quantum-classical boundary can be probed in collisions of bright solitons in Bose-Einstein condensates, where thousands of atoms form a large compound object at ultra cold temperatures. We show that these collisions exhibit intricate quantum-many-body physics, invalidating mean field theory. Prior to collision, solitons can lose their well defined quantum phase relation through phase diffusion, essentially caused by atom number fluctuations. This dephasing should typically render the subsequent dynamics more classical. Instead, we find that it opens the door for a tremendous proliferation of mesoscopic entanglement: After collision the two solitons find themselves in a superposition state of various constituent atom numbers, positions and velocities, in which all these quantities are entangled with those of the collision partner. As the solitons appear to traverse the quantum-classical boundary back and forth during their scattering process, they emerge as natural probe of mesoscopic quantum coherence and decoherence phenomena.

PACS numbers:

*Introduction:* Why most of the world around us follows the classical laws of physics, while being built from quantum mechanical microscopic constituents, is a paramount puzzle of modern physics [1, 2]. As experiments are pushing towards superposition states with more and more constituents [3–12], all points to a central role of decoherence and system-environment entanglement in the transition from quantum to classical appearance [1, 13, 14]. These both inherently rely on the ease with which entanglement proliferates in quantum many body systems.

In ultra-cold gaseous Bose-Einstein condensates (BEC), thousands of atoms can form a compound object, a bright soliton [15], due to their weakly attractive contact interactions. These solitons are localized solutions of the Gross-Pitaevskii equation (GPE) that governs the mean field of the condensate [16–18]. They are protected from dispersion by the non-linearity of atomic interactions, and regularly created since 2002 [18–31], motivated by fundamental studies and applications in atom interferometry [29]. We demonstrate that condensate solitons represent an ideally suited probe to explore the behavior of matter at the quantum classical boundary by exhibiting both, tuneable decoherence and tuneable generation of mesoscopic entanglement.

As opposed to other probes of this boundary, we can continuously change the constituent atom number of a soliton  $N_{\text{sol}}$ , atomic interactions and thus internal soliton structure as well as decoherence. The latter can arise from coupling to an environment, which for cold atomic can be the same type of atoms, hotter and outside of the condensate.

Collisions of classical inert objects are typically fully

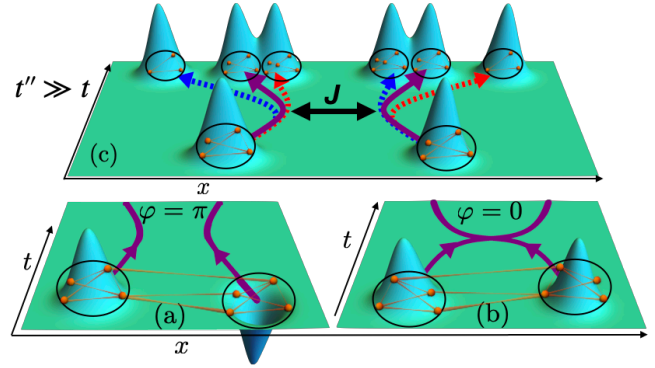


FIG. 1: Soliton collisions near the quantum-classical boundary. (bottom) The collision trajectories (violet lines) of quantum solitons depend crucially on phase coherence (orange lines) of the many-body wave-function. This coherence allows a well defined relative phase,  $\varphi = \pi$  in (a) and  $\varphi = 0$  in (b), between the left and right soliton, controlling collisions. (c) On longer time scales, initial number fluctuations cause a loss of this coherence and the mean collision trajectory (violet) ceases to be dependent on the initial relative phase. However due to atom transfer  $J$  during the collision, solitons subsequently are in a many-body superposition state of various positions as sketched in the figure. For each position, also momentum and atom-number are entangled with those of the collision partner, as sketched by lines of different color, see also Eq. (5).

described by positions and momenta of collision partners. Quantum mechanically, collisions might additionally depend on the quantum phases in the many-body wave function. The latter also play a central role in condensate soliton collisions, which in mean field theory are

controlled by the relative phase  $\varphi$  and distance  $d$  between the colliding solitons. We write their mean-field wave function as

$$\phi(x) = L(x)e^{ikx} + e^{i\varphi}R(x)e^{-ikx}, \quad (1)$$

with left and right soliton shapes  $L(x) = \mathcal{N} \operatorname{sech}[(x + d/2)/\xi]$ ,  $R(x) = \mathcal{N} \operatorname{sech}[(x - d/2)/\xi]$ , where  $\mathcal{N}$  normalises each soliton to contain  $N_{\text{sol}} = \int dx |L(x)|^2 = \int dx |R(x)|^2$  constituent atoms. The soliton widths are set by the healing length scale  $\xi$  and  $k$  is the wave number associated with symmetric bulk soliton motion. In the following we chose units and parameters for which  $\xi = 1$ ,  $\hbar = 1$  and the atomic mass  $m = 1$ . We then draw  $|\phi(x)|^2$  in the inset of Fig. 2 (a).

In mean field theory, solitons evolve through the GPE

$$i \frac{\partial}{\partial t} \phi(x, t) = \left[ -\frac{1}{2} \frac{\partial^2}{\partial x^2} + U_0 |\phi(x, t)|^2 \right] \phi(x, t), \quad (2)$$

with 1D interaction strength  $U_0 = 2a_s(\hbar\omega_\perp) < 0$ , where  $a_s$  is the scattering length and  $\omega_\perp$  the transverse trapping frequency. For a simplified description, the Ansatz (1) can be inserted into (2) yielding effective kinetic equations [32–34] for the time evolving soliton separation  $d(t)$ , velocity  $v(t) = k(t)$  and relative phase  $\varphi(t)$ . Then we see that a relative phase  $\varphi = 0$  yields attractive and  $\varphi = \pi$  repulsive behaviour [32, 33], as sketched in Fig. 1.

However, experiments under different conditions [20, 22–24] portray a mixed picture of the validity of mean-field theory [33, 35–37]. Further, simulations found modifications of soliton interactions by quantum field effects [35, 38]. Here we trace these back to two fundamental processes at play in collisions of many-body solitons: (i) phase diffusion of each individual soliton and (ii) atom transfer between colliding solitons. Combining insight from these basic physical processes involved, we finally predict entanglement of atom-number and soliton momentum resulting from collisions. Thus the many-body quantum dynamics of soliton collisions represents a unique example where the loss of inter-soliton phase coherence actually leads to subsequent enhancement of quantum effects in their collision properties. In a companion article, we show that this picture is consistent with all existing experimental results, and in fact helps to clarify several open questions [34].

*Soliton trains fragment due to phase diffusion:* We now move beyond mean field theory, using: (i) a two-mode-model (TMM) for the atomic quantum field  $\hat{\Psi}(x, t) = \bar{L}[x, d(t)]\hat{a}(t) + \bar{R}[x, d(t)]\hat{b}(t)$ , where  $\hat{a}$  destroys a boson in the left soliton, with *mode* function  $\bar{L}(x) = L(x)/\sqrt{N_{\text{sol}}}$ , and  $\hat{b}$  does the same for the right soliton. Each atom can thus be either in the left or the right soliton (Fig. 1). The mode functions depend on time through the inter-soliton separation  $d(t)$ . (ii) The Multi-Configurational Time Dependent Hartree for Bosons (MCTDHB) [39] with two orbitals based on the package [40], which differs from (i)

by self-consistently evolving also the two mode functions instead of assuming a fixed Ansatz.

The TMM is governed by the Hamiltonian [34]  $\hat{H} = \hat{J}[d(t)](\hat{b}^\dagger \hat{a} + \hat{a}^\dagger \hat{b}) + \frac{\chi}{2}(\hat{a}^\dagger \hat{a}^\dagger \hat{a} \hat{a} + \hat{b}^\dagger \hat{b}^\dagger \hat{b} \hat{b})$  where  $\chi = U_0 \int dx |\bar{L}(x)|^4 = -\frac{mU_0^2 N_{\text{sol}}}{6\hbar^3} < 0$  and  $\hat{J}[d(t)]$  is an operator describing atom transfer between the solitons, which vanishes for large separation  $d(t)$ , see [41].

A measure of whether the two soliton modes are phase coherent is now provided by the two eigenvalues  $(2N_{\text{sol}})\lambda_\pm$  of the one-body density matrix (OBDM) [17, 42, 43], given by

$$\varrho = \begin{bmatrix} \langle \hat{a}^\dagger \hat{a} \rangle & \langle \hat{b}^\dagger \hat{a} \rangle \\ \langle \hat{a}^\dagger \hat{b} \rangle & \langle \hat{b}^\dagger \hat{b} \rangle \end{bmatrix}. \quad (3)$$

If  $\varrho$  has one dominant eigenvalue  $\lambda_+ \approx 1$ , all the atoms reside in the same *single* particle state (orbital), which can represent *two solitons* with complete phase coherence as in (1). Otherwise the system is fragmented with no phase-coherence between solitons [17, 38, 44], hence  $\langle \hat{a}^\dagger \hat{b} \rangle = 0$ .

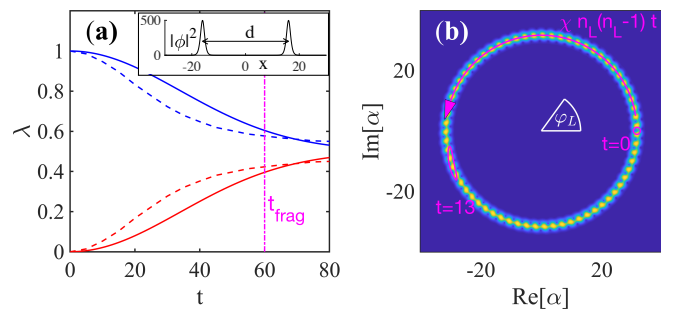


FIG. 2: Phase diffusion fragments bright BEC solitons. (a) Relative occupation  $\lambda$  of all system orbitals at zero temperature in MCTDHB (dashed) and two-mode model (solid). Initially we have a pure BEC of two solitons since  $\lambda = 1$  for one orbital. We call the system fragmented after  $t_{\text{frag}}$ , when  $|\lambda_+(t_{\text{frag}}) - \lambda_-(t_{\text{frag}})| = 0.2$ . The non-linear parameter described in the text is  $\chi = -6.6 \times 10^{-4}$ . The inset shows the initial mean field density  $|\phi|^2$  of the two solitons. (b) Phase diffusion can be visualised through the Husimi Q-function [45]  $Q(\alpha) = |\langle \alpha | \Psi_L \rangle|^2$  of the left soliton's internal state  $|\Psi_L\rangle$  for the same case as (a). Here  $|\alpha\rangle$  is a coherent state centered on  $\alpha \in \mathbb{C}$ . We show  $Q(\alpha)$  at  $t = 50$  where the phase has become undefined and the two solitons fragmented. Half maximum contours of  $Q(\alpha)$  at the earlier times  $t = 0, 13$  are added in magenta. In the space of  $\alpha$ , farther from the origin corresponds to larger atom number  $n_L$ , and the argument indicates the soliton phase  $\varphi_L$ . Thus, the radial width of the Q-function shown represents the uncertainty in atom number of a single soliton, while the angular width implies uncertainty in phase.

Let us initially consider a pair of non-interacting solitons with  $N_{\text{sol}} = 1000$  atoms, placed far apart  $d(t) \equiv 32 = \text{const}$  such that  $\hat{J} = 0$ , see inset Fig. 2 (a). We can then analytically find the time-evolution in the TMM, starting from both solitons in a coherent state (pure

BEC), allowing us to extract the relative occupation  $\lambda_{\pm}$  of the two system orbitals and hence degree of fragmentation as

$$\lambda_{\pm} = \frac{1 \pm e^{2N_{\text{sol}}[\cos(\chi t/\hbar)-1]}}{2} \approx \frac{1 \pm e^{-(t/t_{\text{frag}})^2}}{2}, \quad (4)$$

where the expression after  $\approx$  is valid for short times. The system fragments on the timescale  $t_{\text{frag}} = \hbar/(\sqrt{N_{\text{sol}}}|\chi|)$ . On this timescale the TMM agrees with the substantially more involved MCTDHB method, as shown in Fig. 2 (a).

The model now allows us to trace the physical origin of fragmentation to the ubiquitous phase-diffusion [46–48] of a Bose-gas: To allow a well-defined relative phase between solitons initially, we must have an uncertainty of atom number in each, as in a two-mode or relative coherent state. Due to atom collisions described by the terms  $\sim \chi$  in  $\hat{H}$ , states with a higher number of atoms in, e.g., the left soliton,  $n_L$ , will experience a faster phase evolution  $\exp[-i\chi n_L(n_L - 1)t]$ . In Fig. 2 (b) this implies a faster rotation of the Q-function for larger radial distance from the center, causing the profile shear at  $t = 13$  and then leading to complete phase uncertainty at  $t = 50$ . At that stage a relative phase between solitons can no longer be defined.

While phase-diffusion is ubiquitous in BEC, its detailed dynamics will depend on the number statistics of the initial two-soliton state [46, 49, 50], and thus be quite sensitive to the soliton preparation procedure, e.g. its noisiness [51]. By clearly identifying phase diffusion as the physical cause of soliton train fragmentation, we however show that fragmentation is robust and unavoidable but also frequently slower than experimental time scales. For example using parameters of the experiment [24], one would find a fragmentation time of  $t_{\text{frag}} = 877$  ms.

*Atom transfer in soliton collisions:* Moving to colliding solitons, we now show how fragmentation and collisions affect each other. For this, we again compare TMM and MCTDHB, where the inter-soliton distance  $d(t)$  for the TMM is adjusted to the mean one provided by MCTDHB. We shall separate the fragmentation and collision time-scales by forcing solitons to collide at a set time  $t_{\text{coll}} = |d_{\text{ini}}/(2v_{\text{ini}})|$ , where  $d$  and  $v_{\text{ini}}$  are their initial distance and velocity. We find that prior to fragmentation, solitons collide as predicted by mean-field theory (2) dependent on their relative phase. Here MCTDHB soliton trajectories agree with the effective kinetic equation of motion for  $d(t)$ , shown as teal lines, see Fig. 3 (a,c).

We however see that the attractive collision has *increased* the degree of fragmentation in panel (b), which should otherwise only fragment at  $t_{\text{frag}} \approx 60$ . We find that this is due to atoms transferring from one soliton to the other when these are close, as they inevitably become when interactions are attractive. Transfer through the  $\hat{J}$  terms are then possible during a short time interval only, forming an intermittent Bosonic-Josephson-Junction (BJJ) [52]. The transfer “pulse” *non-adiabatically* widens

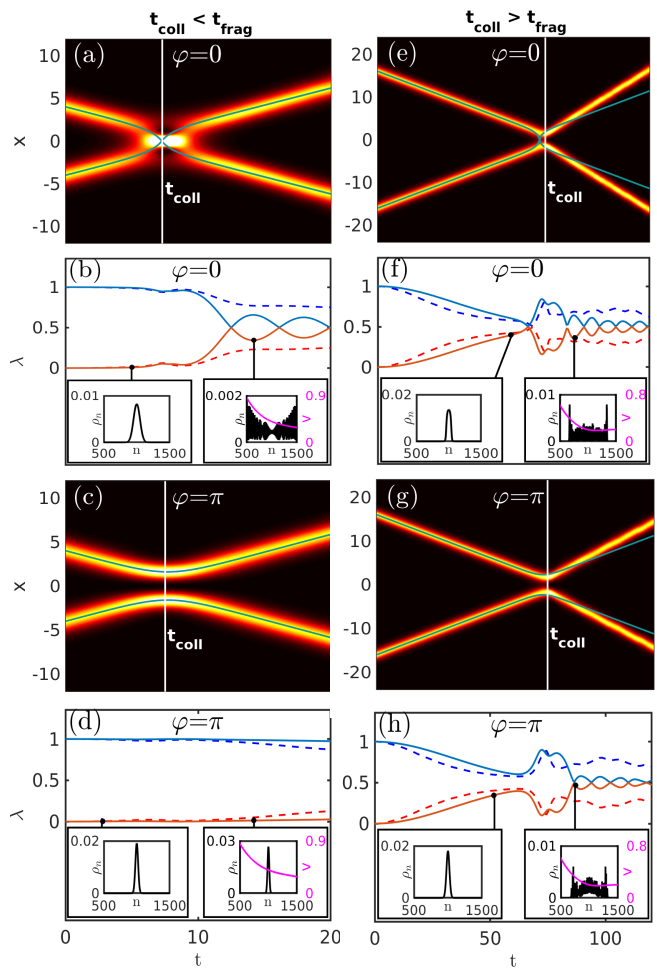


FIG. 3: Collision and coherence dynamics in controlled soliton collisions, before fragmentation, at time  $t_{\text{coll}} < t_{\text{frag}}$  (a-d) and after fragmentation, at time  $t_{\text{coll}} > t_{\text{frag}}$  (e-h). The initial relative phases between solitons,  $\varphi$ , are indicated. (a,c,e,g) Total atomic density from MCTDHB and expected mean-field trajectories based on Eq. (2) (teal line). (b,d,f,h) The two largest orbital populations  $\lambda(t)$  from MCTDHB (dashed) and the two mode model (solid). For the latter we used a time-dependent soliton separation  $d(t)$ , which is inferred from the MCTDH peak densities. The insets show, for one of the solitons, the pre- and post-collision atom number probabilities  $\rho_n$  from the TMM (black), at the indicated time ( $\bullet$ ). The magenta line is the outgoing soliton velocity  $v(n)$  for a soliton with  $n$  atoms after the collision.

the atom number distribution  $\rho_n$ , shown in the inset. A wider number distribution then leads to faster phase diffusion in subsequent dynamics. The effect is absent in the repulsive case of panel (d), due to much less atom transfer. Note that the TMM is expected to quantitatively fail in the attractive case as the two mode functions become identical when  $d = 0$ . Nonetheless the qualitative feature of increased fragmentation is also evident in MCTDHB. We thus conclude that attractive collisions will cause earlier subsequent fragmentation.

When quantum solitons collide after fragmentation,

$t_{\text{coll}} > t_{\text{frag}}$ , almost no initial phase-dependence of collision trajectories remains in the mean atomic density provided by MCTDHB, see Fig. 3 (e,g). Collisions always seem to have repulsive character. They also appear super-elastic, with solitons gaining kinetic energy in the collision, while total energy is conserved. We propose the following explanation: the MCTDHB method provides a variationally optimised approximation within its two-mode constraint, to describe a massively entangling quantum many body collision beyond its reach.

We can see how the latter must arise from basic principles: The short opportunity for atomic transfers between solitons causes a much larger spread of the atom number distribution in a soliton than before the collision, shown in the inset of Fig. 3 (f,h). This effect is much more pronounced in collisions after fragmentation than those before, compare panel (d). It is accompanied by a partial restoration of phase coherence (or de-fragmentation), in panels (f,h), in accordance with number and phase being conjugate variables. Due to transfer during the collision, the two solitons may significantly differ in atom number after the collision. Let us denote the number of atoms in the left (right) soliton after collision with  $n_{\text{left}}$  ( $n_{\text{right}}$ ) and assume incoming solitons had velocities  $\pm v_0$  and fixed atom number  $n_0 = N_{\text{sol}}$ . If atoms now have transferred from one soliton to the other, momentum and energy conservation prohibit symmetric outgoing soliton velocities  $\pm v_0$ , and instead dictate the velocity of the left soliton  $v(a)$  as a function of number asymmetry  $a = (n_{\text{left}} - n_{\text{right}})/2$ , see [41]. Averaging this velocity (magenta line in the insets) over the probabilities of a certain asymmetry,  $p_{n_{\text{left}}}$  (black line in the insets), this can *quantitatively* account for the mean kinetic energy gain through a drop of internal energy, as we show in [34].

The emergent picture now involves entanglement of post-collision momentum with relative atom number. The post-collision many-body state, sketched in Fig. 1 (c) then has the schematic structure

$$|\Psi_{\text{pc}}\rangle = \sum_a c_a |N_{\text{sol}} + a, v(a)\rangle_L \otimes |N_{\text{sol}} - a, v(-a)\rangle_R, \quad (5)$$

if we ignore the initial number fluctuations. The states  $|n, v\rangle$  in Eq. (5) indicate the constituent number  $n$  and velocity  $v$  (hence also position) of the left and right soliton separately and  $c_a$  are complex coefficients. The schematic (5) constitutes the many-body generalisation of semi-classical results [53] and is also reminiscent of the collision induced two species Bell states proposed in [54] and entanglement generation involving dark [55] or dark-bright solitons [56].

While neither of our methods can capture the final state (5), they are expected to correctly describe the two robust features of quantum soliton dynamics, which then necessitate this final state: (i) phase diffusion that is present in any condensate with number fluctuations and

(ii) Josephson type tunnelling that would be present in any well defined two-mode system with contact between the modes.

We show in the companion article [34] that fragmentation is accelerated in a heated condensates and how the theory developed here is consistent with experiments [20, 22–24] and further helps to reconcile seemingly contradictory earlier results regarding the applicability of mean field theory.

*Conclusions and outlook:* We have connected fragmentation of solitons to phase diffusion, which allows us to predict the fragmentation time scale. Since phase diffusion causes a loss of coherence between two solitons, it initially appears like a de-coherence process. However, while this renders the mean of collisions more classical, namely independent of an initial inter-soliton quantum phase, it in fact enhances subsequent proliferation of entanglement: At the moment of collision, we have shown strong interplay between the bulk soliton kinematics and two-mode many body physics. This leads to partial re-coherence during the collision but subsequent entanglement of atom-number and momentum in a soliton.

Their well understood internal many-body structure [54, 57, 58], yet rich emergent many body physics now make BEC solitons an ideal probe of the quantum to classical boundary: How does the intricately entangled post collision state manifest itself in a single experimental observation? How does it respond to de-coherence at finite temperature? Can we treat internal phase and number variables of the solitons as an environment for their bulk position and momentum variables? In the absence of a comprehensive many-mode, many-body, thermal quantum theory, experiments will have to answer many of those questions. As we have shown, collisions themselves will be a useful diagnostic of many-body dynamics, complementing interferometry [59].

We stress that even if a thermal environment has washed out inter-soliton quantum effects, each soliton still requires internal quantum coherence and entanglement [60] to maintain its structure. The present system will thus allow to explore also internal interactions that are able to preserve local quantum coherence despite the presence of an environment, preserving quantum bound states.

*Acknowledgments:* We gladly acknowledge the Max-Planck society for funding under the MPG-IISER partner group program, and interesting discussions with T. Busch, S. Cornish, M. Davis, S. Gardiner, J. Hope and C. Weiss. ASR acknowledges the Department of Science and Technology (DST), New Delhi, India, for the INSPIRE fellowship IF160381.

- 
- [1] M. Schlosshauer, *Rev. Mod. Phys.* **76**, 1267 (2005).
- [2] M. A. Schlosshauer, *Decoherence and the quantum-to-classical transition* (Springer, 2007).
- [3] J. R. Friedman, V. Patel, W. Chen, S. Tolpygo, and J. E. Lukens, *nature* **406**, 43 (2000).
- [4] W.-B. Gao, C.-Y. Lu, X.-C. Yao, P. Xu, O. Gühne, A. Goebel, Y.-A. Chen, C.-Z. Peng, Z.-B. Chen, and J.-W. Pan, *Nature physics* **6**, 331 (2010).
- [5] D. Leibfried, E. Knill, S. Seidelin, J. Britton, R. B. Blakestad, J. Chiaverini, D. B. Hume, W. M. Itano, J. D. Jost, C. Langer, et al., *Nature* **438**, 639 (2005).
- [6] H. Takahashi, K. Wakui, S. Suzuki, M. Takeoka, K. Hayasaka, A. Furusawa, and M. Sasaki, *Phys. Rev. Lett.* **101**, 233605 (2008).
- [7] S. Gerlich, S. Eibenberger, M. Tomandl, S. Nimmrichter, K. Hornberger, P. J. Fagan, J. Tüxen, M. Mayor, and M. Arndt, *Nature communications* **2**, 263 (2011).
- [8] C.-Y. Lu, X. Zhou, O. Ghne, W.-B. Gao, J. Zhang, Z.-S. Yuan, A. Goebel, T. Yang, and J.-W. Pan, *Nature Physics* **3** (2006).
- [9] C. Monroe, D. M. Meekhof, B. E. King, and D. J. Wineland, *Science* **272**, 1131 (1996).
- [10] M. Arndt, O. Nairz, J. Vos-Andreae, C. Keller, G. van der Zouw, and A. Zeilinger, *Nature* **401**, 680 (1999).
- [11] M. Arndt and K. Hornberger, *Nature Physics* **10**, 271 (2014).
- [12] S. Eibenberger, S. Gerlich, M. Arndt, M. Mayor, and J. Tüxen, *Phys. Chem. Chem. Phys.* **15**, 14696 (2013).
- [13] L. Hackermüller, K. Hornberger, B. Brezger, A. Zeilinger, and M. Arndt, *Nature* **427**, 711 (2004).
- [14] K. Hornberger, S. Uttenthaler, B. Brezger, L. Hackermüller, M. Arndt, and A. Zeilinger, *Phys. Rev. Lett.* **90**, 160401 (2003).
- [15] Technically the BEC solitons in question are solitary waves throughout this article.
- [16] Y. S. Kivshar and G. P. Agrawal, *Optical Solitons: From Fibers to Photonic Crystals* (Academic, San Diego, 2003).
- [17] C. J. Pethick and H. Smith, *Bose-Einstein condensation in dilute gases* (Cambridge University Press, 2002).
- [18] K. E. Strecker, G. B. Partridge, A. G. Truscott, and R. G. Hulet, *New Journal of Physics* **5**, 73 (2003).
- [19] L. Khaykovich, F. Schreck, G. Ferrari, T. Bourdel, J. Cubizolles, L. D. Carr, Y. Castin, and C. Salomon, *Science* **296**, 1290 (2002).
- [20] K. E. Strecker, G. B. Partridge, A. G. Truscott, and R. G. Hulet, *Nature* **417**, 150 (2002).
- [21] B. Eiermann, T. Anker, M. Albiez, M. Taglieber, P. Treutlein, K.-P. Marzlin, and M. K. Oberthaler, *Phys. Rev. Lett.* **92**, 230401 (2004).
- [22] S. L. Cornish, S. T. Thompson, and C. E. Wieman, *Phys. Rev. Lett.* **96**, 170401 (2006).
- [23] J. H. V. Nguyen, D. Luo, and R. G. Hulet, *Science* **356**, 422 (2017).
- [24] J. H. V. Nguyen, P. Dyke, D. Luo, B. A. Malomed, and R. G. Hulet, *Nature Physics* **10**, 918 (2014).
- [25] A. L. Marchant, T. P. Billam, M. M. H. Yu, A. Rakonjac, J. L. Helm, J. Polo, C. Weiss, S. A. Gardiner, and S. L. Cornish, *Phys. Rev. A* **93**, 021604(R) (2016).
- [26] A. L. Marchant, T. P. Billam, T. P. Wiles, M. M. H. Yu, S. A. Gardiner, and S. L. Cornish, *Nature Comm.* **4**, 1865 (2013).
- [27] P. Medley, M. A. Minar, N. C. Cizek, D. Berryrieser, and M. A. Kasevich, *Phys. Rev. Lett.* **112**, 060401 (2014).
- [28] S. Lepoutre, L. Fouché, A. Boissé, G. Berthet, G. Salomon, A. Aspect, and T. Bourdel, *Phys. Rev. A* **94**, 053626 (2016).
- [29] G. D. McDonald, C. C. N. Kuhn, K. S. Hardman, S. Bennetts, P. J. Everitt, P. A. Altin, J. E. Debs, J. D. Close, and N. P. Robins, *Phys. Rev. Lett.* **113**, 013002 (2014).
- [30] P. J. Everitt, M. A. Sooriyabandara, M. Guasoni, P. B. Wigley, C. H. Wei, G. D. McDonald, K. S. Hardman, P. Manju, J. D. Close, C. C. N. Kuhn, et al., *Phys. Rev. A* **96**, 041601(R) (2017).
- [31] T. Mežnaršič, T. Arh, J. Brencelj, J. Pišljarič, K. Gosar, i. c. v. Gosar, R. Žitko, E. Zupanič, and P. Jeglič, *Phys. Rev. A* **99**, 033625 (2019), URL <https://link.aps.org/doi/10.1103/PhysRevA.99.033625>.
- [32] J. P. Gordon, *Opt. Lett.* **8**, 596 (1983).
- [33] U. Al-Khawaja, H. T. C. Stoof, R. G. Hulet, K. E. Strecker, and G. B. Partridge, *Phys. Rev. Lett.* **89**, 200404 (2002).
- [34] S. Choudhury, A. Sreedharan, R. Mukherjee, A. Streltsov, and S. Wüster (2019), <http://arxiv.org/abs/1904.11878>.
- [35] B. J. Dąbrowska-Wüster, S. Wüster, and M. J. Davis, *New Journal of Physics* **11**, 053017 (2009).
- [36] L. D. Carr and J. Brand, *Phys. Rev. Lett.* **92**, 040401 (2004).
- [37] L. Salasnich, A. Parola, and L. Reatto, *Phys. Rev. Lett.* **91**, 080405 (2003).
- [38] A. I. Streltsov, O. E. Alon, and L. S. Cederbaum, *Phys. Rev. Lett.* **106**, 240401 (2011).
- [39] O. E. Alon, A. I. Streltsov, and L. S. Cederbaum, *Phys. Rev. A* **77**, 033613 (2008).
- [40] K. Sakmann, A. U. J. Lode, A. I. Streltsov, O. E. Alon, and L. S. Cederbaum, *Openmctdhhb v2.3* (2012), <http://OpenMCTDHB.uni-hd.de>.
- [41] See Supplemental Material at [URL will be inserted by publisher] for details on the two-mode model and post-collision soliton velocities.
- [42] O. Penrose and L. Onsager, *Phys. Rev. A* **104**, 576 (1956).
- [43] P. B. Blakie and M. J. Davis, *Phys. Rev. A* **72**, 063608 (2005).
- [44] E. J. Mueller, T. L. Ho, M. Ueda, and G. Baym, *Phys. Rev. A* **74**, 033612 (2006).
- [45] D. F. Walls and G. J. Milburn, *Quantum Optics* (Springer Verlag, 1994).
- [46] M. Lewenstein and L. You, *Phys. Rev. Lett.* **77**, 3489 (1996).
- [47] C. Menotti, J. R. Anglin, J. I. Cirac, and P. Zoller, *Phys. Rev. A* **63**, 023601 (2001).
- [48] S. A. Haine, *New Journal of Physics* **20**, 033009 (2018).
- [49] J. A. Dunningham, M. J. Collet, and D. F. Walls, *Phys. Lett. A* **245**, 49 (1998).
- [50] M. Haque and A. E. Ruckenstein, *Phys. Rev. A* **74**, 043622 (2006).
- [51] M. J. Edmonds, T. P. Billam, S. A. Gardiner, and T. Busch, *Phys. Rev. A* **98**, 063626 (2018).
- [52] M. Albiez, R. Gati, J. Fölling, S. Hunsmann, M. Cristiani, and M. K. Oberthaler, *Phys. Rev. Lett.* **95**, 010402 (2005).
- [53] M. Lewenstein and B. A. Malomed, *New Journal of Physics* **11**, 113014 (2009).

- [54] B. Gertjerenken, T. P. Billam, C. L. Blackley, C. R. Le Sueur, L. Khaykovich, S. L. Cornish, and C. Weiss, Phys. Rev. Lett. **111**, 100406 (2013).
- [55] R. V. Mishmash and L. D. Carr, Phys. Rev. Lett. **103**, 140403 (2009).
- [56] G. C. Katsimiga, G. M. Koutentakis, S. I. Mistakidis, P. G. Kevrekidis, and P. Schmelcher, New J. Phys. **19**, 073004 (2017).
- [57] C. Weiss and Y. Castin, Phys. Rev. Lett. **102**, 010403 (2009).
- [58] C. Weiss and Y. Castin, Journal of Physics A: Mathematical and Theoretical **45**, 455306 (2012).
- [59] J. L. Helm, S. J. Rooney, C. Weiss, and S. A. Gardiner, Phys. Rev. A **89**, 033610 (2014).
- [60] J. C. Zill, T. M. Wright, K. V. Kheruntsyan, T. Gasenzer, and M. J. Davis, SciPost Phys. **4**, 011 (2018).

**SUPPLEMENTAL INFORMATION: SOLITONS  
EXPLORE THE QUANTUM CLASSICAL  
BOUNDARY**

*Complete Two-mode model:* The position dependent terms omitted in the main article are:

$$\begin{aligned} \hat{H} = & E_0(\hat{a}^\dagger \hat{a} + \hat{b}^\dagger \hat{b}) + \frac{\chi}{2}(\hat{a}^\dagger \hat{a}^\dagger \hat{a} \hat{a} + \hat{b}^\dagger \hat{b}^\dagger \hat{b} \hat{b}) \\ & + J(\hat{b}^\dagger \hat{a} + \hat{a}^\dagger \hat{b}) + \bar{U}(4\hat{a}^\dagger \hat{a} \hat{b}^\dagger \hat{b} + \hat{a}^\dagger \hat{a}^\dagger \hat{b} \hat{b} + \hat{b}^\dagger \hat{b}^\dagger \hat{a} \hat{a}) \\ & + 2\bar{J}(\hat{a}^\dagger \hat{a} + \hat{b}^\dagger \hat{b} - 1)(\hat{b}^\dagger \hat{a} + \hat{a}^\dagger \hat{b}), \end{aligned} \quad (6)$$

with coefficients

$$E_0 = \int dx \bar{L}(x) \left[ -\frac{\hbar^2}{2m} \frac{\partial^2}{\partial x^2} \right] \bar{L}(x), \quad (7)$$

$$\chi = U_0 \int dx \bar{L}(x)^4 = -\frac{mU_0^2 N_{\text{sol}}}{6\hbar^3}, \quad (8)$$

$$J = \int dx \bar{L}(x) \left[ -\frac{\hbar^2}{2m} \frac{\partial^2}{\partial x^2} \right] \bar{R}(x), \quad (9)$$

$$\bar{U} = \frac{U_0}{2} \int dx \bar{L}(x)^2 \bar{R}(x)^2, \quad (10)$$

$$\bar{J} = \frac{U_0}{2} \int dx \bar{L}(x)^3 \bar{R}(x). \quad (11)$$

*Number-momentum entanglement:* An equal number of atoms,  $N_{\text{sol}}$ , are contained in the two incoming solitons with momenta  $p_0$  and  $-p_0$  per atom, thus the initial total net momentum is zero.

At the moment of collision, due to close proximity of solitons tunnelling is likely. Let us assume  $a$  atoms are transferred from the left to the right soliton. If we denote the outgoing momenta per atom by  $p_+$  and  $-p_-$ , conservation of momentum requires:

$$(N_{\text{sol}} + a)p_+ - (N_{\text{sol}} - a)p_- = 0. \quad (12)$$

Together with energy conservation

$$\begin{aligned} N_{\text{sol}} \frac{p_0^2}{m} + \chi N_{\text{sol}}^2 = & (N_{\text{sol}} + a) \frac{p_+^2}{2m} + \chi \frac{(N_{\text{sol}} + a)^2}{2} \\ & + (N_{\text{sol}} - a) \frac{p_-^2}{2m} + \chi \frac{(N_{\text{sol}} - a)^2}{2}, \end{aligned} \quad (13)$$

the equations (12) can be solved to yield momenta of atoms in outgoing solitons  $p_{\pm}$ .

We find

$$p_+ = \pm \frac{\sqrt{a - N_{\text{sol}}} \sqrt{a^2 m \chi - p_0^2 N_{\text{sol}}}}{\sqrt{a N_{\text{sol}} + N_{\text{sol}}^2}}. \quad (14)$$

with matching velocities  $v = p_+/m$  shown in Fig. 3.